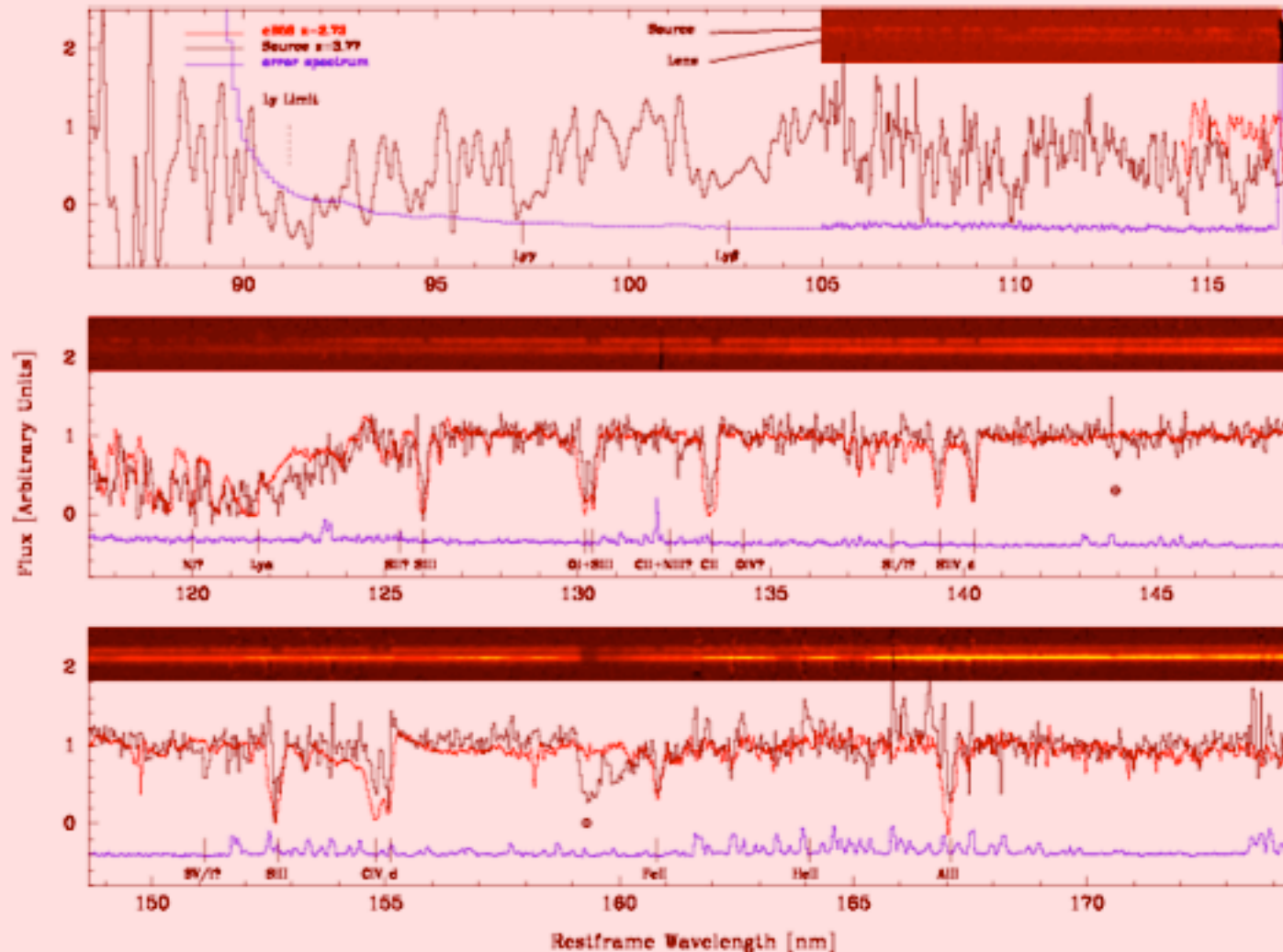


High-redshift galaxies

Probing the ISM of a Starburst Galaxy at $z = 3.8$ with medium-resolution spectroscopy

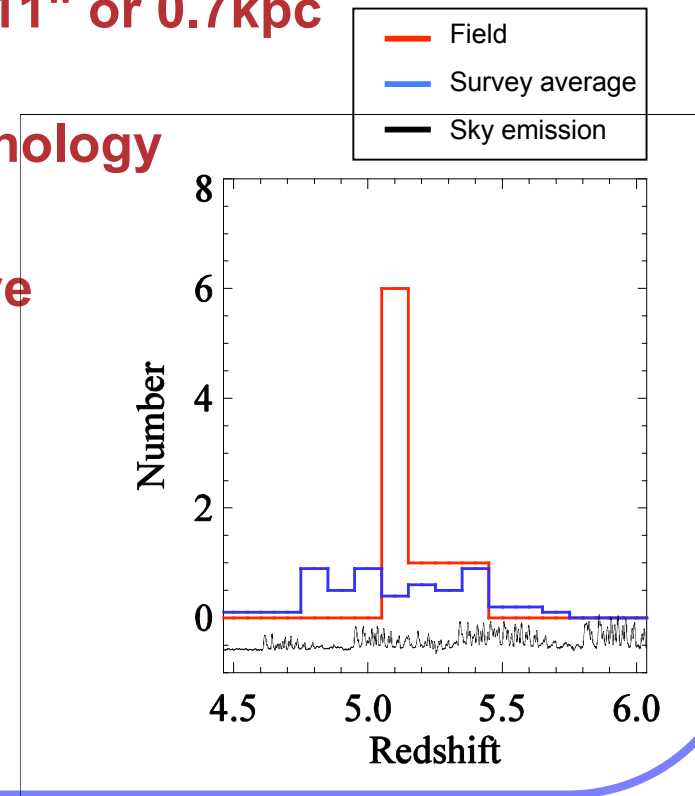
R. CABANAC (LATT), D. VALLS-GABAUD (GEPI), C. LIDMAN (ESO), L. CHRISTENSEN (ESO)



Galaxies at $z \sim 5$: Small, Clustered & Colourful P23

Laura Douglas (Observatoire de Paris), Malcolm Bremer (Uni. Bristol),
Matt Lehnert (Observatoire de Paris), Elizabeth Stanway (Uni. Bristol)

- **36 Lyman- α line emitting & 28 Lyman Break galaxies**
 - line fluxes from 5×10^{-18} to 7×10^{-17} ergs $\text{cm}^{-2} \text{s}^{-1}$
- **Typical galaxy compact with $R_{1/2} = 0.11''$ or 0.7kpc**
- **26% of galaxies show complex morphology**
- **2 fields have redshift spikes indicative of large scale structure**
- **LBGs and weak line emitters have redder UV continuum than strong line emitters**



No. 24 H. Kajino(Kyoto Univ.) Ly α rest EW vs rest UV absolute luminosity

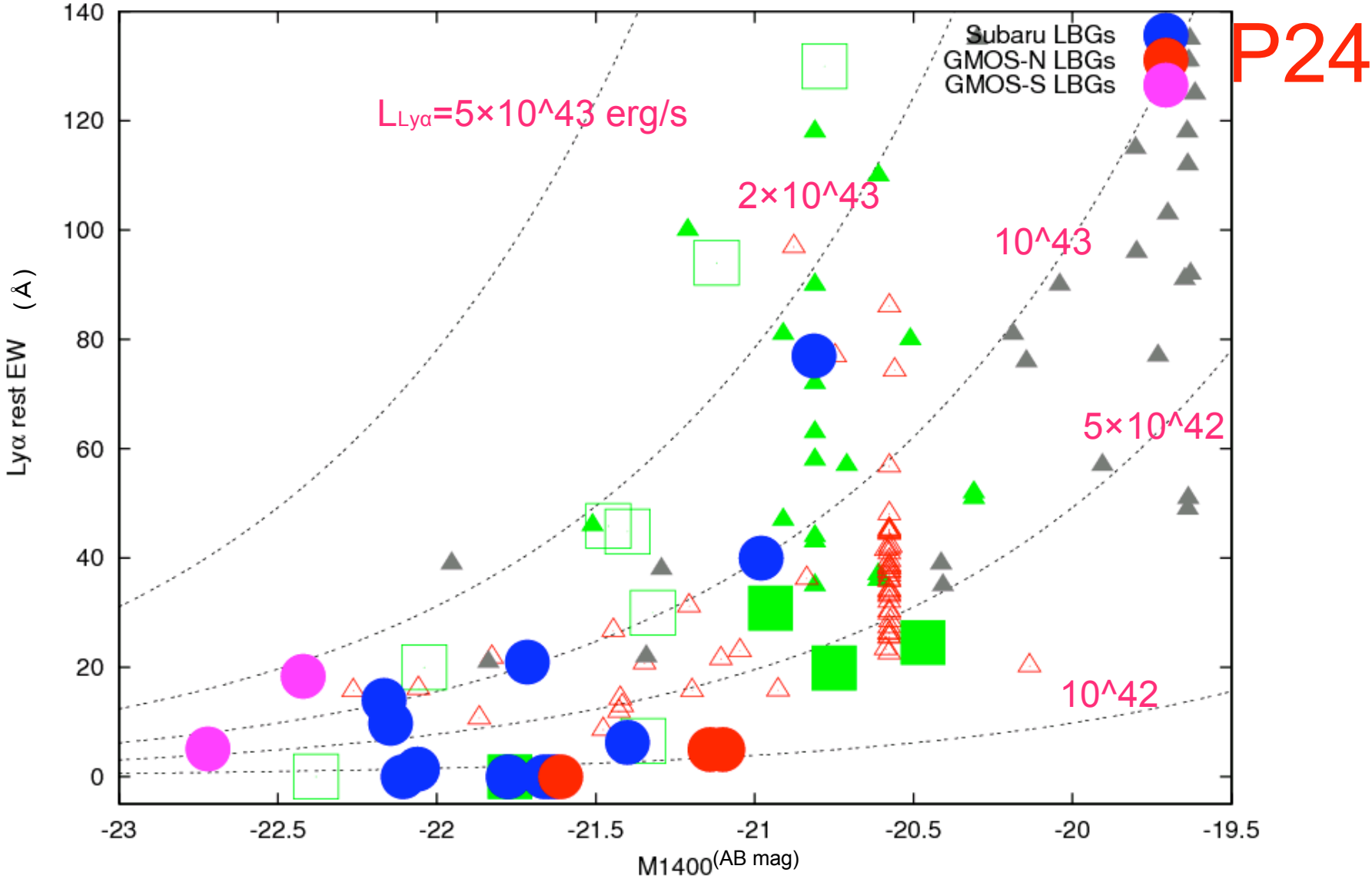


Fig. 5. Filled circles show our spectroscopic $z \sim 5$ sample. Filled squares, open squares, filled triangles and open triangles show $z \sim 5$ LBGs, $z \sim 6$ LBGs, $z \sim 5.7$ LAEs and 6.6 LAEs from literature, respectively. This figure suggests the deficiency of UV luminous LBGs with large Ly α EW.

Looking for the first galaxies: lensing or blank fields?

P25

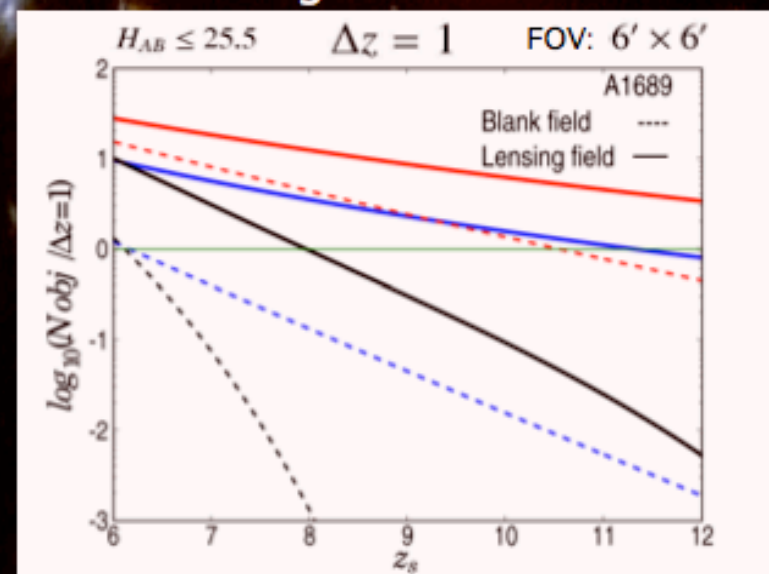
Context : Identification and study of the first galaxies in lensing clusters

Aims : This work is intended to discuss the relative efficiency of lensing and blank fields in the identification and study of sources at $6 < z < 12$.

Its aim is to determine the best possible observing strategies in order to build up a representative sample of spectroscopically confirmed $z > 6$ galaxies.

Main conclusions :

- Lensing clusters improve the survey efficiency by a factor $\sim 5 - 10^2$ depending on source LF.
- The most efficient lensing clusters are at moderate redshift ($z \sim 0,1 - 0,3$).
- Important variance effect for spectroscopic depths ($\sim 25,5$ AB).
- Blank fields are needed to constrain the bright-end of the LF.
- Observing different lensing clusters allows us to constrain the LF.

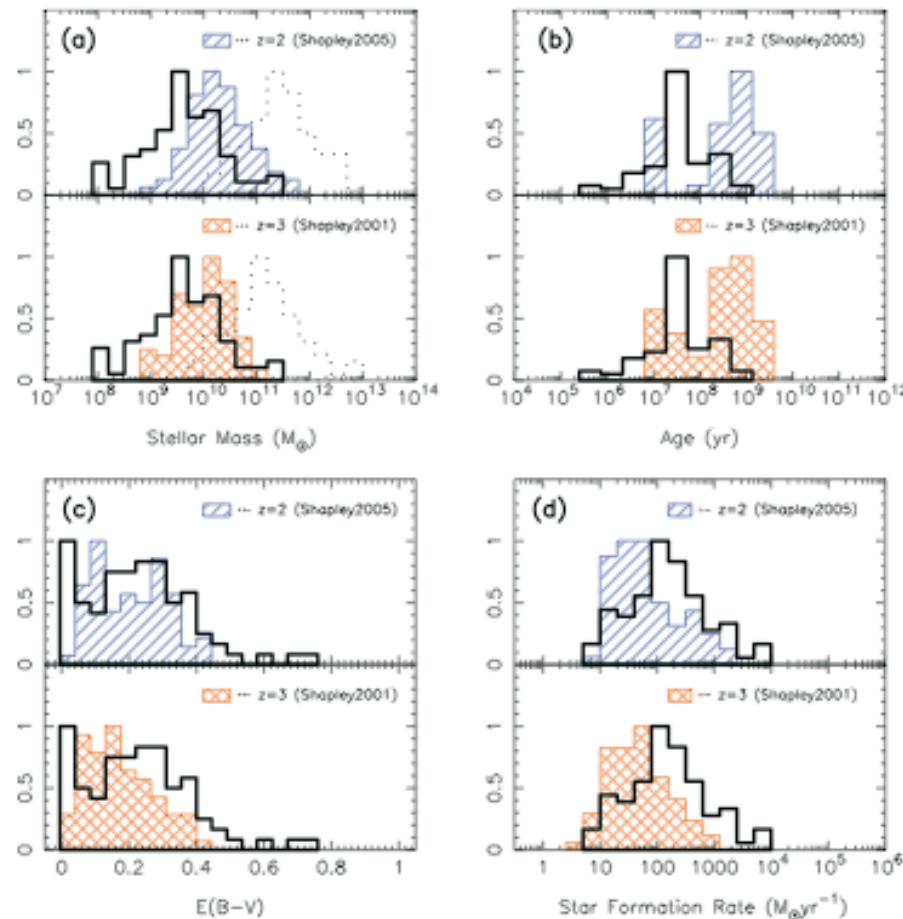


$\langle z \rangle = 4.0$	$\alpha = 1.6,$	$\phi^* = 1.3 \cdot 10^{-3} \text{ Mpc}^{-3},$	$M^* = -21.07$	Steidel et al. (1999)
$\langle z \rangle = 5.9$	$\alpha = 1.74,$	$\phi^* = 1.1 \cdot 10^{-3} \text{ Mpc}^{-3},$	$M^* = -20.24$	Bouwens et al. (2006)
$3.8 < z < 7.4$	$\alpha = 1.74,$	$\phi^* = 1.1 \cdot 10^{-3} \text{ Mpc}^{-3},$	$M^* = -21.02 + 0.36(z - 3.8)$	Bouwens et al. (2008)

P27 K. Ohta

Stellar populations of LBGs at $z \sim 5$ I: The stellar masses, ages, color excesses and star formation rates

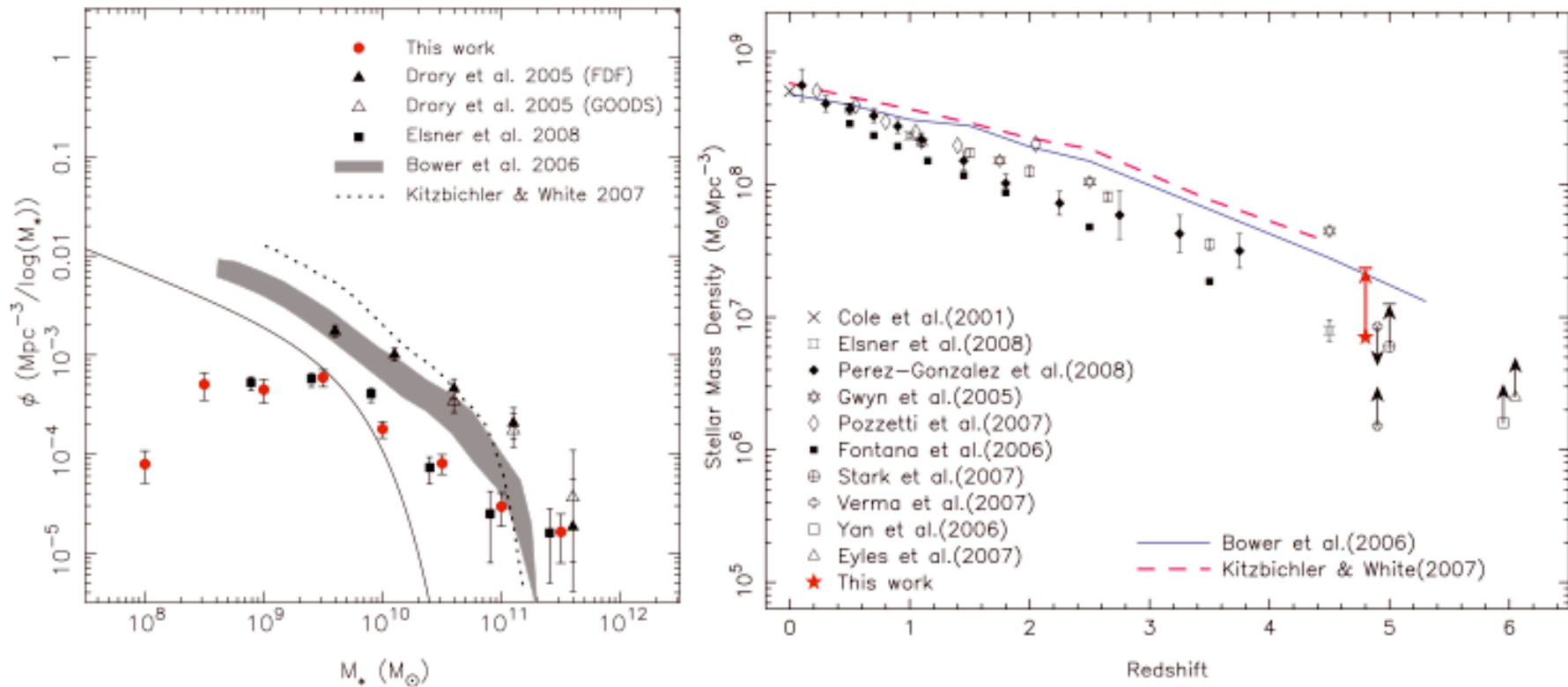
P27



Distributions of best-fitted parameters for $z \sim 5$ sample with that for $z=3$ sample from Shapley et al.(2001) and $z=2$ sample from Shapley et al.(2005). For comparison, peaks of the distribution are normalized to unity. The stellar mass of $z \sim 5$ galaxies is smaller than that of $z=2-3$ galaxies by a factor of ~ 4 . The age of $z \sim 5$ galaxies is relatively younger than that of $z=2-3$ galaxies and the star formation rate is higher than in $z=2-3$.

P30 K.Yabe

Stellar populations of LBGs at $z \sim 5$ II: The stellar mass function and the stellar mass density



Left: Comparison of the stellar mass function of LBGs at $z \sim 5$ with other observations and theoretical predictions of semi-analytic models. Our stellar mass function is indicated by red circles. **Right:** The cosmic stellar mass density as a function of redshift. Our result is indicated by a red star and plausible upper limit is shown with a horizontal bar.

P30

The L- σ relation for HII galaxies

Eduardo Telles*

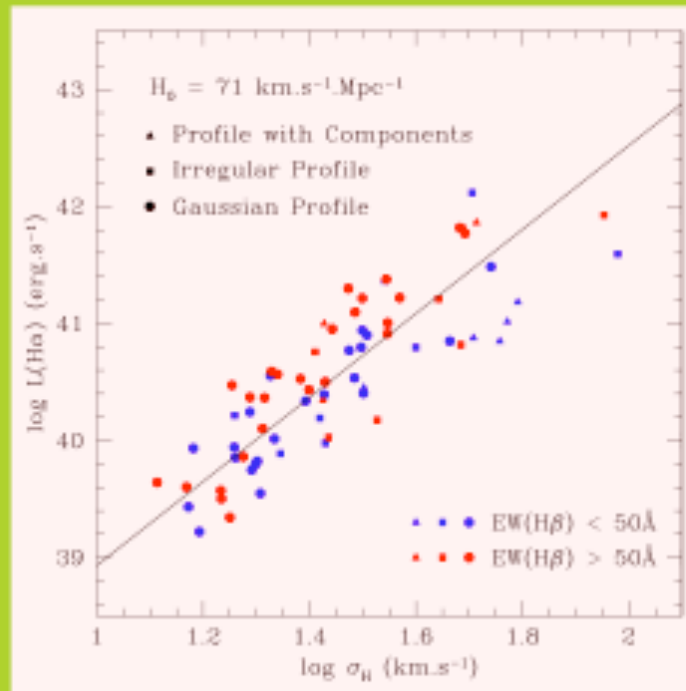
Dept. of Astronomy, Univ. of Virginia, Charlottesville, VA, USA

*Observatório Nacional - Rio de Janeiro - Brazil



$$L(\text{H}\beta) \propto \sigma^4$$

*Correlation or Upper Envelope?
Fundamental Plane?*



Left graph shows the $[L - \sigma]$ relation for 70 galaxies for which we have fluxes and equivalent width $\text{H}\beta$ from Kehrig et al. spectrophotometry. The solid line represents the bi-variate fit linear fit.

$$\log L(\text{H}\alpha) = (3.59 \pm 0.27) \log \sigma + (35.34 \pm 0.38)$$

RMS = 0.38

PCA results:

We used the PCA technique to identify a second parameter in $[L - \sigma]$ relation. Here $\text{EW}(\text{H}\beta)$ appears to be a possible second parameter in $[L - \sigma]$ relation, representing 33.6% of the variability as a second principal component.

P28

Gamma-ray bursts



Host Galaxies of Long Gamma Ray Bursts from a hybrid galaxy formation model



*Campisi Maria Angela - MPA Garching b. Muenchen (Germany)
campisi@mpa-garching.mpg.de
PhD Supervisors: Prof. Rashid Sunyaev & Dr. Li-Xin Li
in collaboration with Dr. Gabriella De Lucia and Prof. Shude Mao.*

I will present an analysis of the LongGRBs host galaxies obtained by coupling high resolution N-body simulations with semi-analytic techniques for modelling the formation and evolution of galaxies.

Results in summary:

- SFR evolution:** . If the triggering of GRBs is suppressed in high metallicity progenitors this is no longer the case and LGRBs became a biased tracer of the cosmic star formation history .
- Mass of Host:** Typical LGRBs host galaxies tend to occupy preferentially the low mass end of the galaxy mass function.
- **Metallicity evolution:** LGRBs host galaxies have typically lower metallicity than the "average" galaxy population at each redshift. The evolution is consistent, within the errors, with observational measurements.
- Correlation function:** From two-point auto-correlation function for LGRBs host galaxies and cross-correlation between host and normal galaxies, we argue that LGRBs host galaxies tend to inhabit regions with lower than average density.
- Evolutionary stage of LGRBs Host Galaxies:** the mass-metallicity relation for LGRBs host galaxies at redshift ~ 4 and evolution of their descendants at lower redshifts, shows as evolve the host with the redshift.

-For the figures and details see the poster n° 31

Campisi M.A., De Lucia G., Li L.X., Mao S., 2008,
in preparation

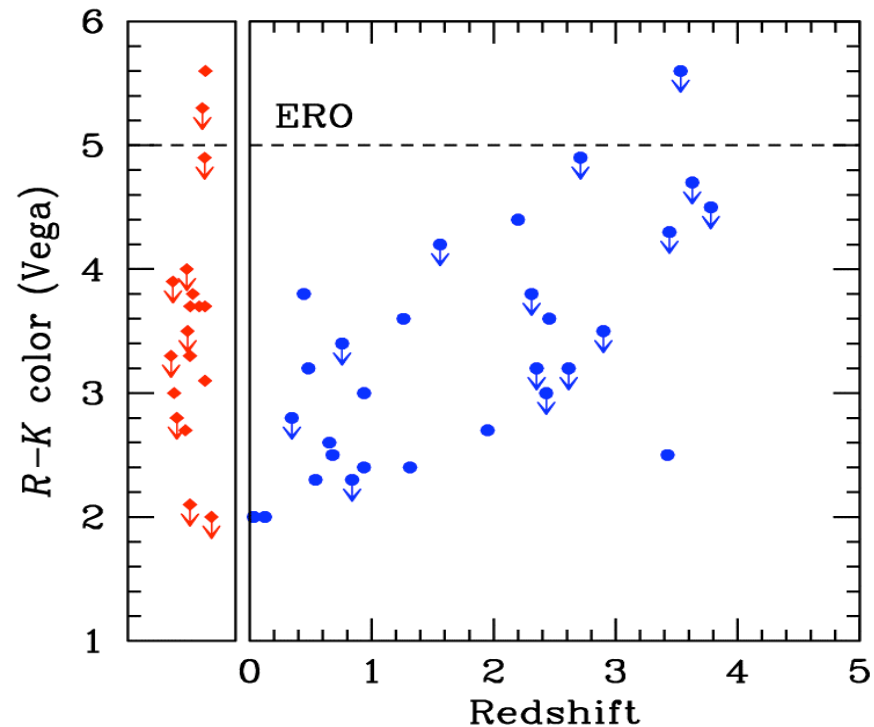
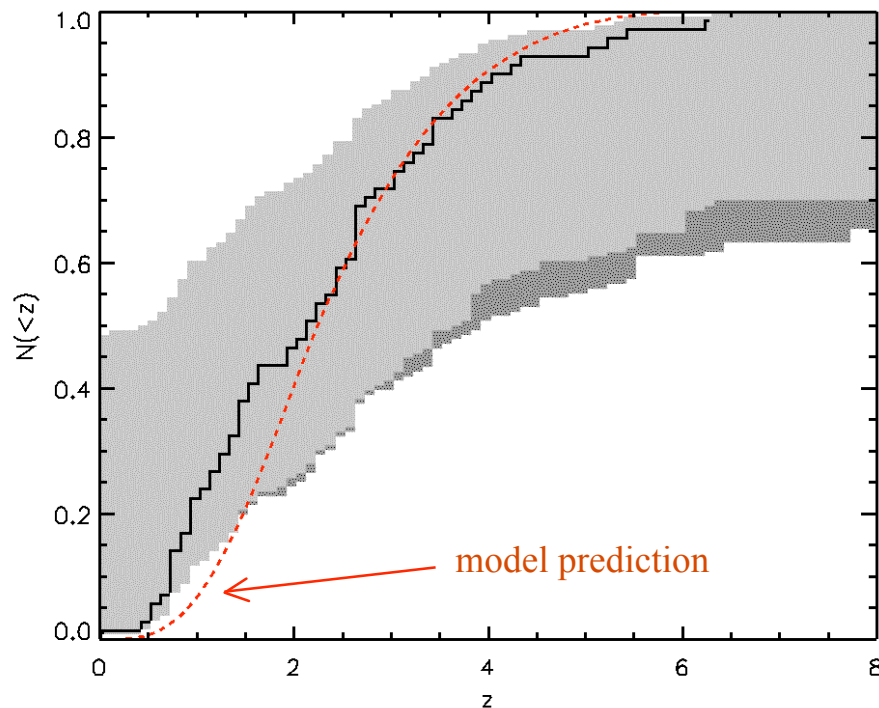
P31

Building a Complete Sample of *Swift* Gamma-Ray Bursts

Palli Jakobsson (University of Hertfordshire)

P32

- Part 1: The aim is to construct a sample that is unbiased towards optically bright afterglows. Crucial for estimating the true GRB redshift distribution with error bars (left figure).
- Part 2: We have a large programme at the VLT (total of 272 hours) to characterize the host galaxies of this homogeneously selected sub-sample of *Swift* GRBs (71 hosts). One of many results show a very small fraction of extremely red objects (right figure).



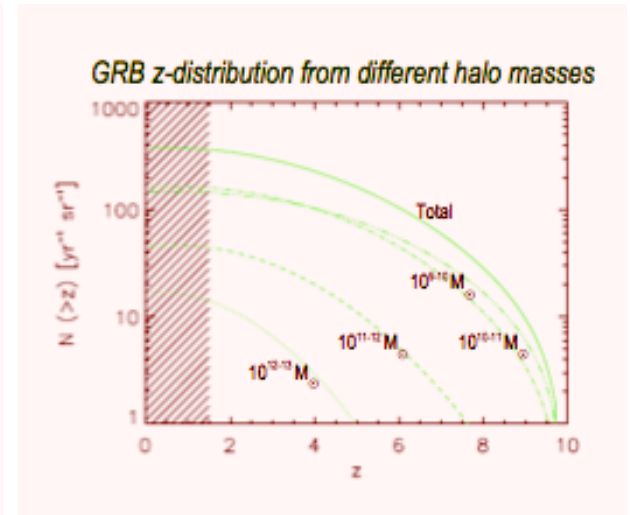
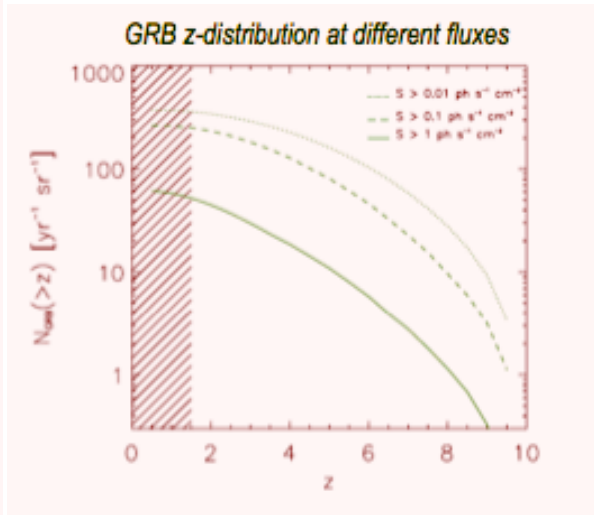
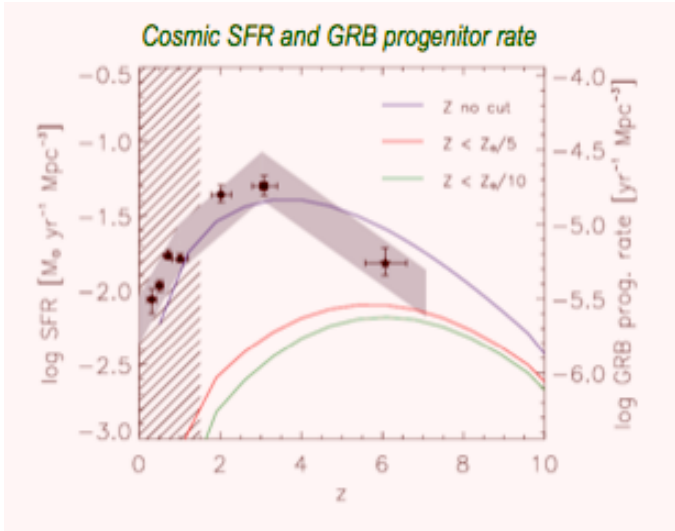


Università degli Studi di Roma "Tor Vergata" (Rome, Italy)

Scuola Internazionale Superiore di Studi Avanzati (Trieste, Italy)

LONG GAMMA-RAY BURSTS AND THEIR HOST GALAXIES AT HIGH REDSHIFT

A. Lapi (UniRoma2/SISSA, Italy)
 N. Kawakatu (NAOJ, Japan)
 Z. Bosnjak (IAP, France)
 A. Celotti (SISSA, Italy)
 A. Bressan (INAF-OAPD, Italy)
 G.L. Granato (INAF-OATS, Italy)
 L. Danese (SISSA, Italy)



QSO absorption lines

P34

C. Ledoux et al.

VLT/UVES spectroscopy of GRB optical afterglows

Molecules in the interstellar medium at high redshift

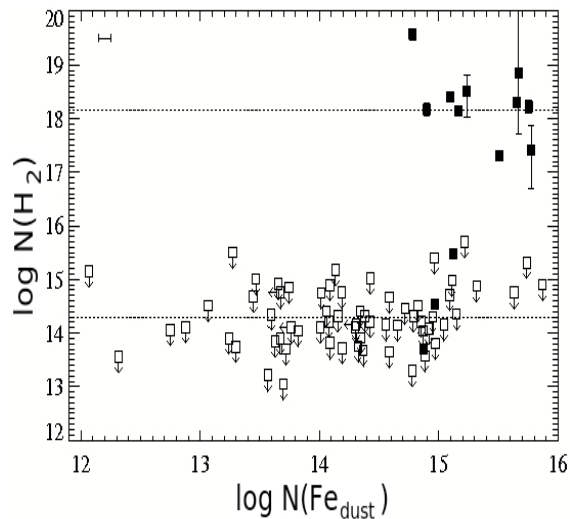
P. Noterdaeme P. Petitjean C. Ledoux R. Srianand

P50

H₂

14 detections in the range
z=1.8-4.3

Presence strongly dependent
on that of dust



Physical conditions in the ISM

- T, n, UV flux
- important self-shielding effects
- shocks? turbulences?

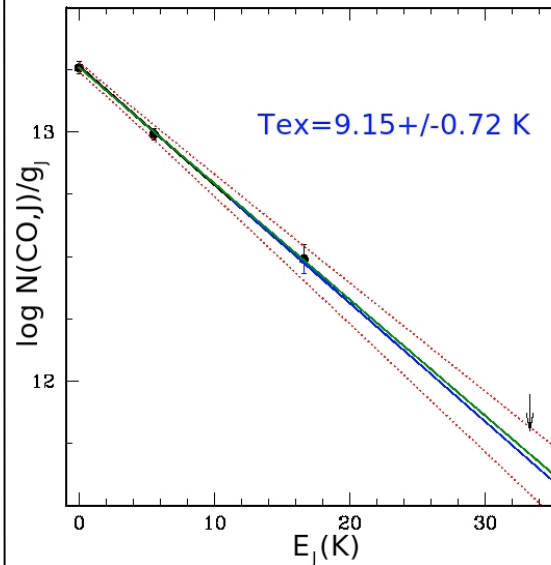
CO

First detection
z=2.4 towards
SDSSJ1439+1117

Solar metallicity DLA

CO/H₂ as in diffuse local ISM

CO rotational levels:
Temperature of the CMB

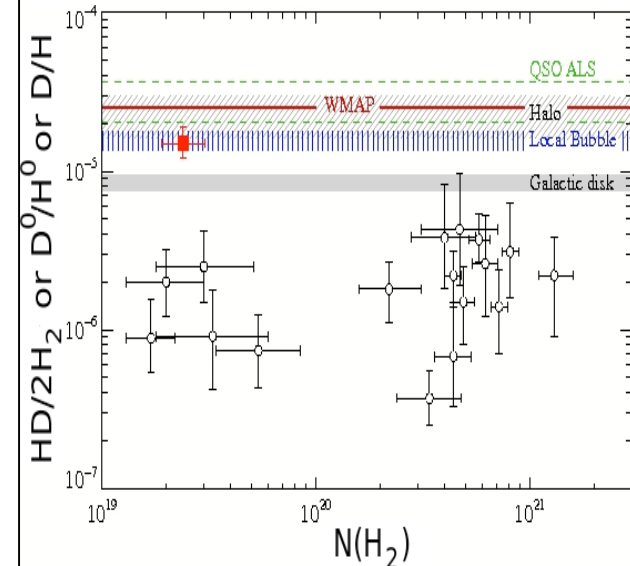


HD

2 detections

Q1439:
D/H > 1/2 primordial
despite of high chemical
enrichment

Intense infall of primordial
gas



P39

A. Aghaee P. Petitjean et al.

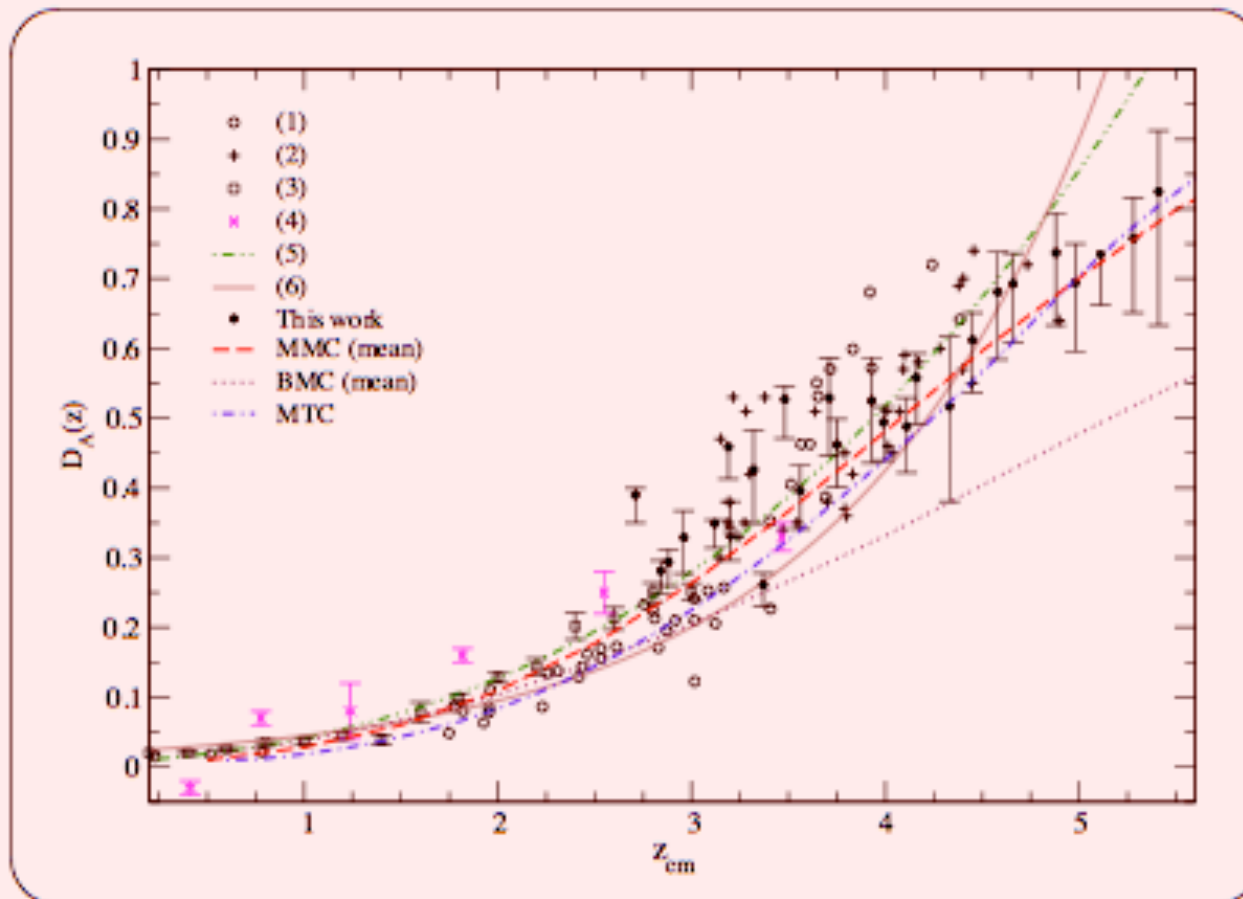
Systematic comparison of high-resolution and low-resolution absorption spectra of the **same** QSOs in order to study systematic uncertainties of continuum fitting.

The Cosmic Flux Decrement: A Consistent Picture?

P44

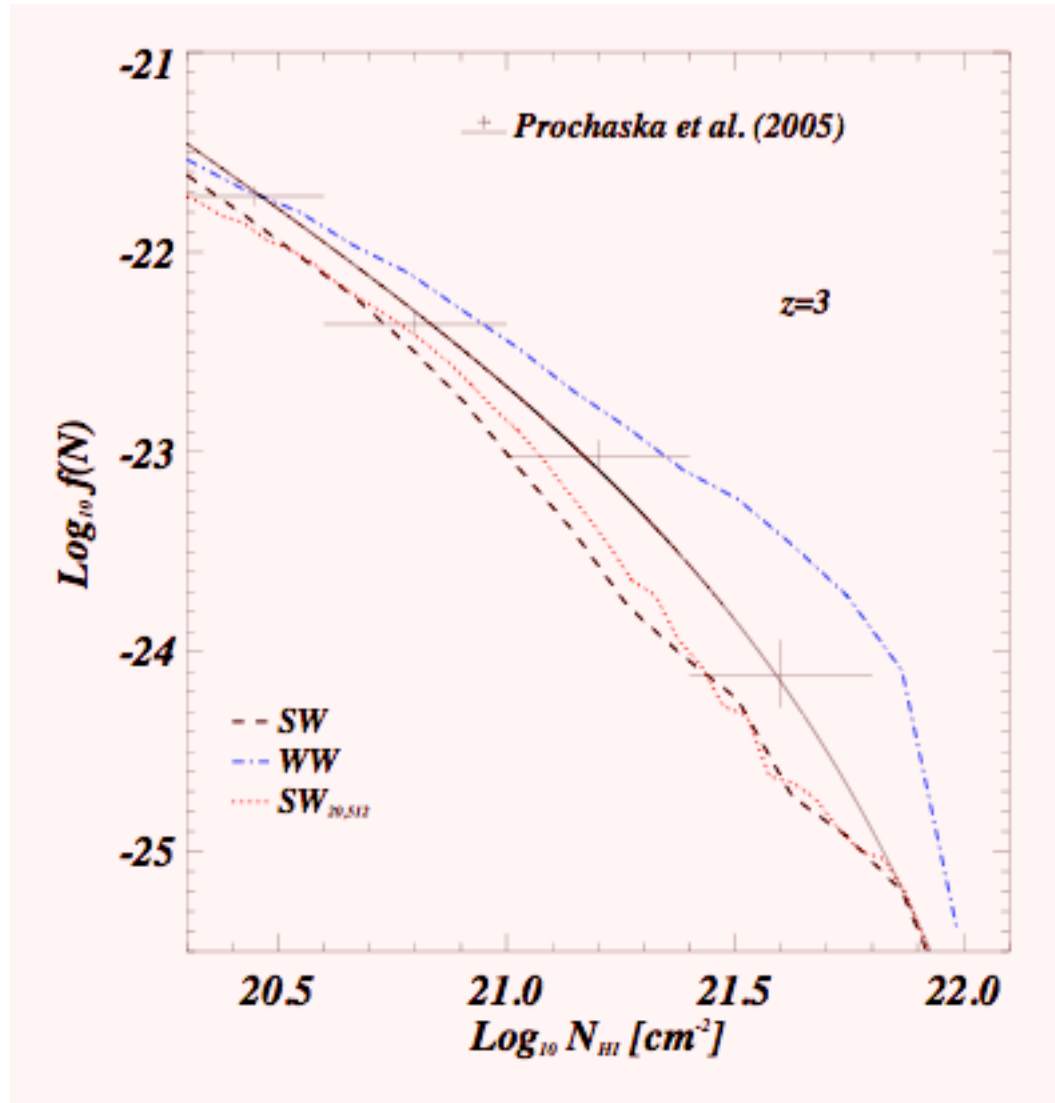
Thorsten Tepper Garcia^{1,2} Uta Fritze³ Philipp Richter¹

¹ Institut für Physik und Astronomie, Universität Potsdam, Germany ² Institut für Astrophysik, Universität Göttingen, Germany ³ Centre for Astrophysics Research, University of Bedfordshire, UK
tepper@astro.physik.uni-potsdam.de



Evolution of the excess D_A for different models: MMC (dashed line), BMC (dotted line), and MTC (dot-dashed line); observations: (1) Zuo & Lu (1993), (2) Schneider et al. (1991), (3) Kirkman et al. (2007), (4) O'Brien et al. (1988); empirical fits: (5) Zhang et al. (1997), (6) Kirkman et al. (2005). All data points display 1 σ error bars.

Properties of DLAS from high-resolution hydro-dynamical simulations



P. Tescari, S.
Borgani, M.
Viel et al.

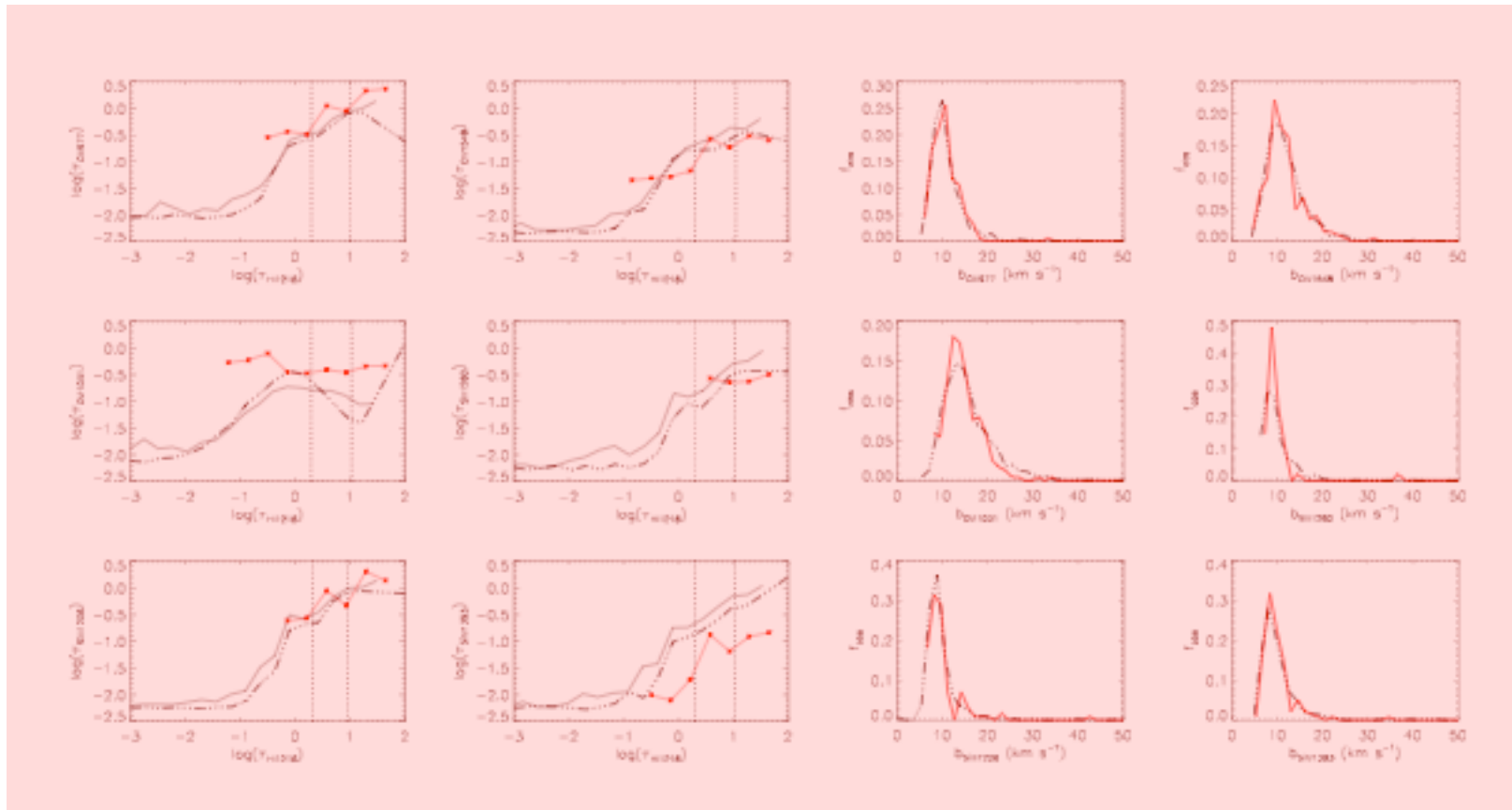
SPH simulation
with strong and
weak winds

P29

Absorption features of high-redshift galactic winds

A. Fangano et al.

P36



Metal absorption in SPH simulations with galactic winds

P37

UV background

A Monte Carlo simulation of the intergalactic absorption and the detectability of the Lyman continuum from distant galaxies

P37

Akio K. Inoue^{1*} and Ikuru Iwata²

¹College of General Education, Osaka Sangyo University, 3-1-1, Nakagaito, Daito, Osaka 574-8530, Japan

²Okayama Astrophysical Observatory, National Astronomical Observatory of Japan, Kamogata, Okayama 719-0232, Japan

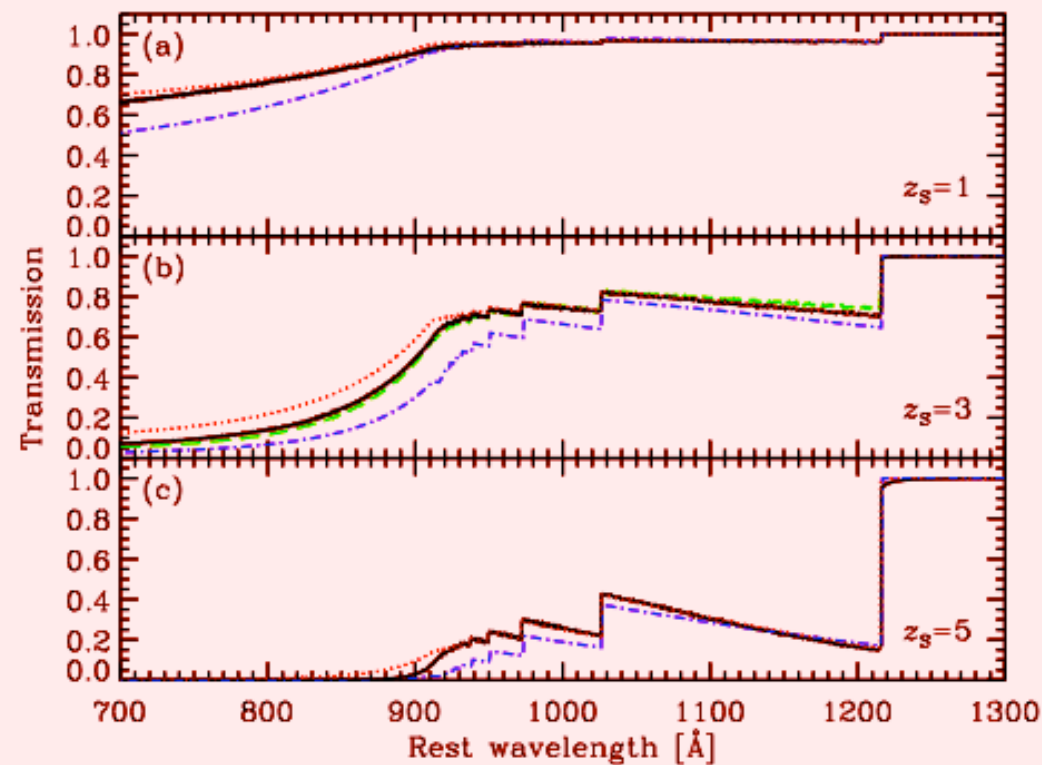
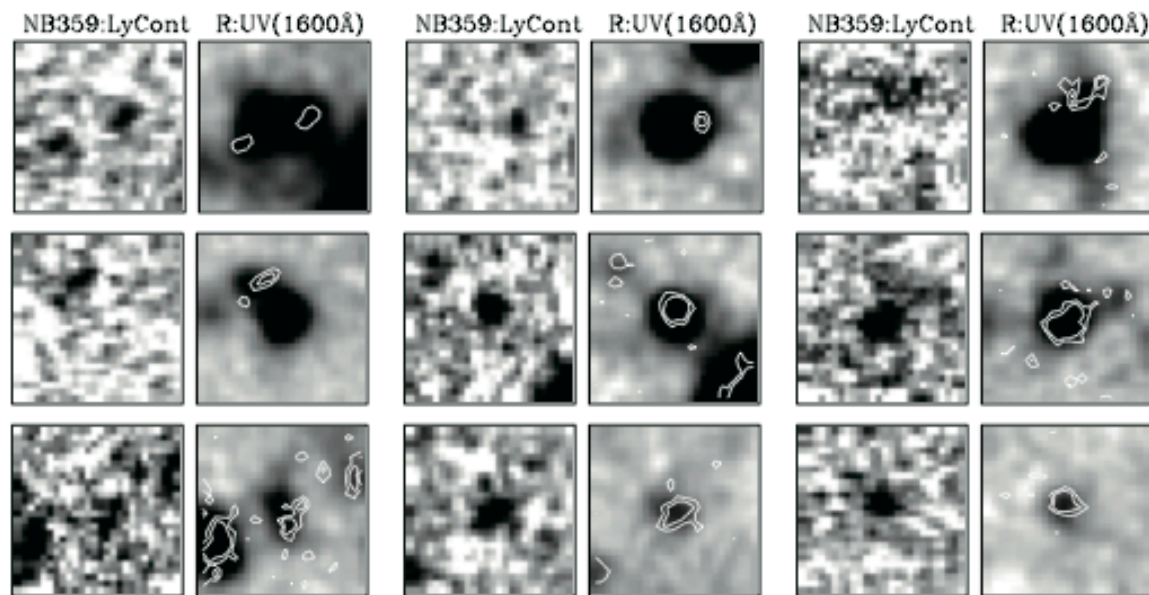


Figure 6. Average IGM transmissions. The horizontal axis is the wavelength in the source rest-frame. The source redshifts are noted in the panels. The solid lines are our Monte Carlo results; 10,000 lines of sight are averaged in each panel. The dot-dashed lines are the mean transmission models of Madau (1995). The dotted lines are the mean transmission models of Meiksin (2006) but the updated version. The dashed line in the panel (c) is the average transmission of the Monte Carlo simulation by Bershadsky et al. (1999) (MC-Kim model).

Ionizing Radiation from Galaxies at $z=3$ through Wide-Field Narrow-Band Imaging

Iwata et al. Poster #38



- 17 Lyman continuum (LyC) Detections out of 198 Galaxies at $z\sim 3.1$

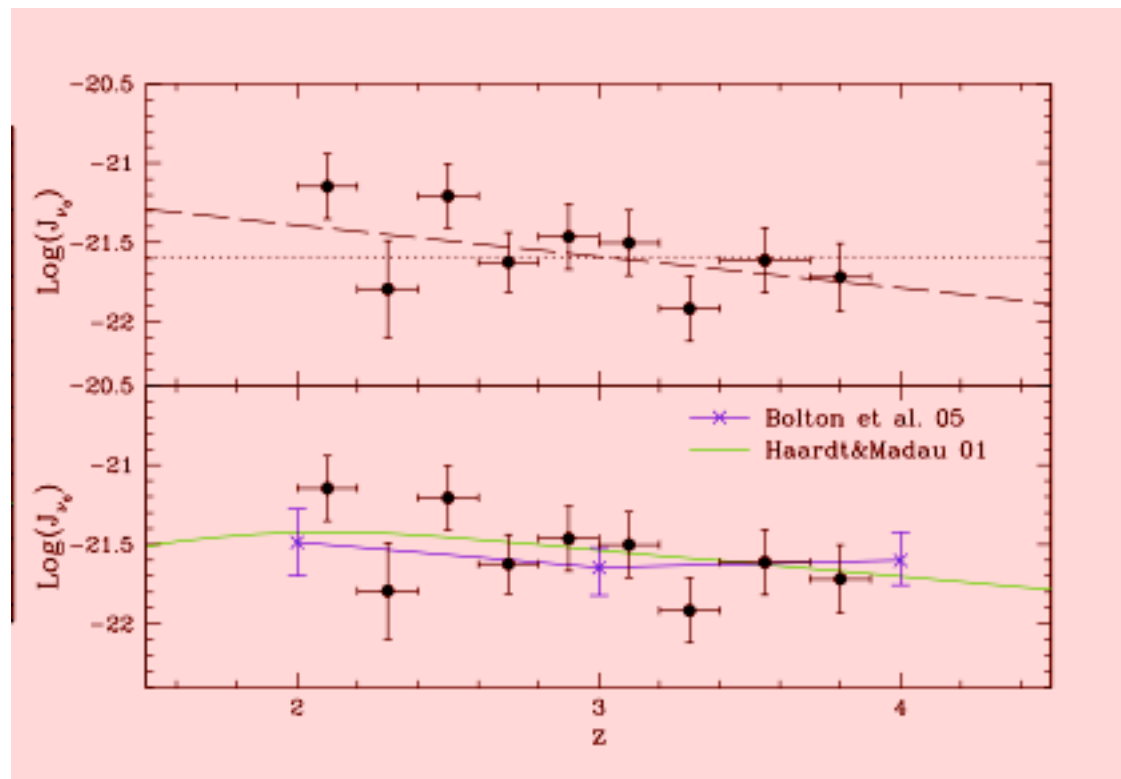
- $f_{\text{LyC}}/f_{\text{UV}}=0.20$ for 7 LBGs
- Blue SED; top heavy IMF?

Examples of postage stamp images of galaxies from which Lyman continuum is detected. Field of view is $5'' \times 5''$.

P38

An unbiased measurement of the UV background and its evolution via the proximity effect statistic

Aldo Dall'Aglio, Gabor Worsack and Lutz Wisotzki
Astrophysikalisches Institut Potsdam



P41

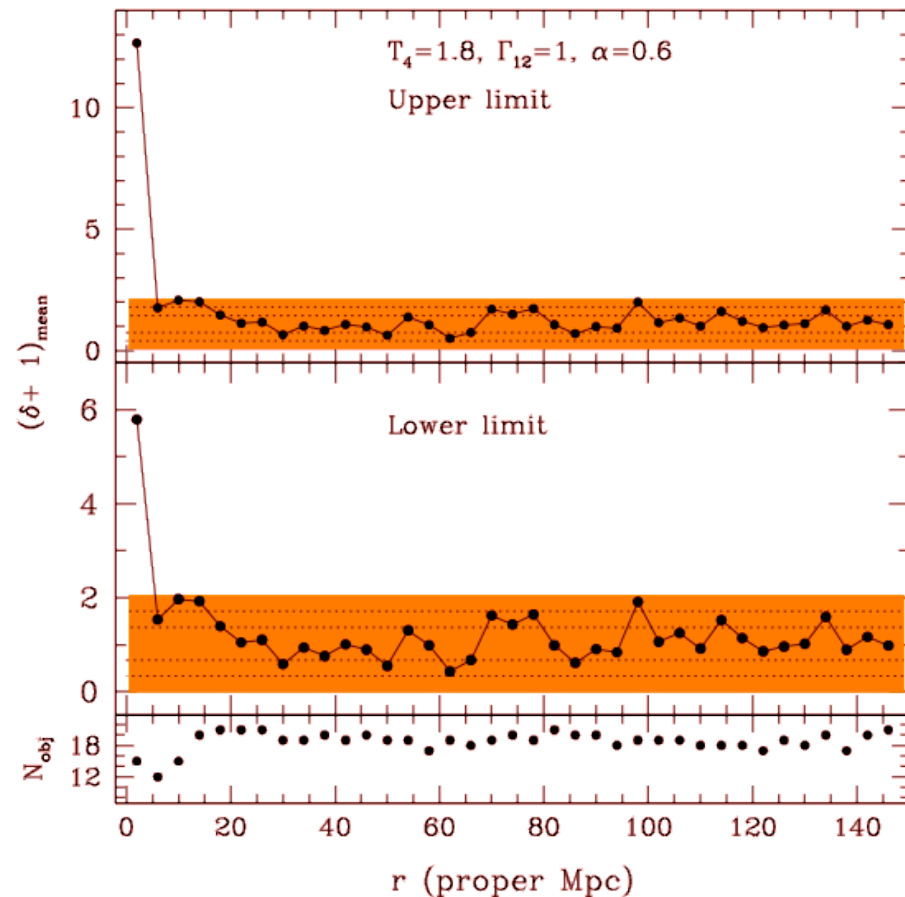
[40] Recovering the density field from QSO absorption lines with FLO P40

V. D'Odorico (dodorico@oats.inaf.it) , F. Saitta, M. Bruscoli, F. Fontanot, M. Viel, S. Cristiani, P. Monaco

FLO (From Lines to Overdensities) is a new technique which allows to directly recover the density field of the IGM as traced by the Ly α forest absorption lines observed in QSO spectra.

The method has been tested against simulated spectra and applied to a sample of 21 observed QSO spectra at high resolution and high S/N.

Figure: the average density field as a function of the proper separation from the QSO, a significant overdensity within 4 proper Mpc is clearly detected.



The Transverse Proximity Effect in Spectral Hardness

G. Worseck, C. Fechner, L. Wisotzki & A. Dall'Aglio

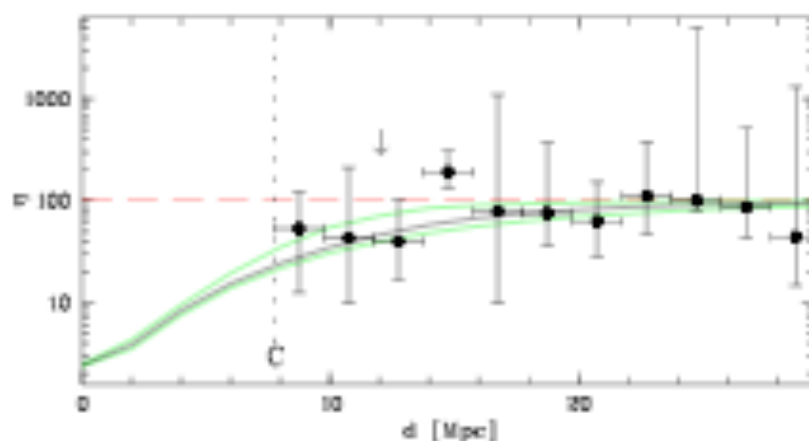


Figure: Average η vs. proper distance between a foreground QSO (C) and the background sightline. Small values of η correspond to hard radiation. Despite large intrinsic fluctuations, the radiation field near the QSO is *on average* harder than the UV background.

- transverse proximity effect: foreground QSO ionizes Ly α forest on background sightline
- so far: existence of effect controversial
- survey for foreground QSOs near known background QSOs
- two lines of sight with intergalactic HeII absorption
 $\rightarrow \eta = N_{\text{HeII}}/N_{\text{HI}}$ measures UV spectral shape along the line of sight
- two lines of sight with intergalactic HeII absorption
 $\rightarrow \eta = N_{\text{HeII}}/N_{\text{HI}}$ measures UV spectral shape along the line of sight
- harder UV radiation in close projection to all 7 foreground QSOs than far away from them
- conclusion: transverse proximity effect detected via a locally harder radiation field
- minimum QSO lifetime 10–30 Myr

P45

E.R. Titley, A. Meiksin

Effects of helium reionization on

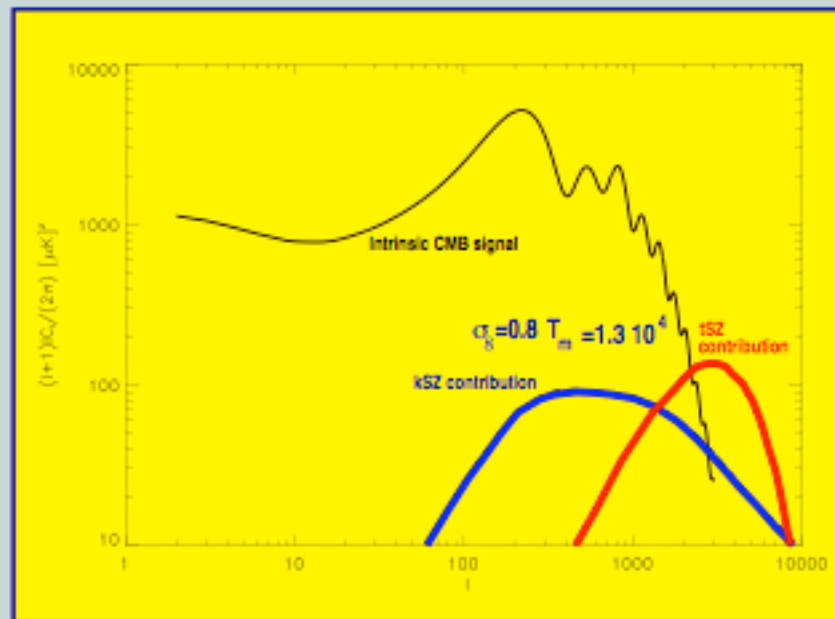
- temperature of IGM and the Doppler parameter distribution of the hydrogen Ly-alpha forest
- hardness of UV background spectrum as determined from comparison of hydrogen and helium Lyman-alpha forest



XXIVth IAP Conference "Far Away: Light in the young Universe"

Probing the State of the IGM via the Thermal and Kinematic SZ-effect

J.P. Mücke¹, F. Atrio-Barandela²



The figure shows the tSZ and kSZ contributions for different parameters. Recent studies show that the WMAP data fit can be improved if adding the kSZ contribution (Atrio-Barandela, Mücke, Genova-Santos 2008) indicating on a possible detection of the kSZ effect.

P42

Lyman-alpha emission

Pierleoni Marco - MPA Garching b.
Muenchen (Germany)
In collaboration with
Benedetta Ciardi &
Antonella Maselli

CRASH α

P43

THE DETECTION AND THE PROPERTY OF $LY-\alpha$ RADIATION FROM A GALAXY DEPENDS ON LOCAL HII REGIONS PRODUCED BY THE IONIZING RADIATION. TO INVESTIGATE THIS ISSUE, WE HAVE JOINED TWO DIFFERENT CODES: ONE DESCRIBES $LY-\alpha$ PHOTONS PROPAGATING THROUGH A GIVEN HYDROGEN DENSITY DISTRIBUTION AND ONE TREATS THE EFFECTS ON THE PHYSICAL CONDITION OF THE GAS DURING THE PROPAGATION OF IONIZING RADIATION. THE MAIN TECHNICAL PROBLEM TO INCLUDE THE TWO RADIATIONS IN THE SAME CODE IS THE TIME TREATMENT. IN FACT THE IONIZING RADIATION IS CHARACTERIZED BY A CONTINUOUS ABSORPTION ALONG ITS PATH, WHILE $LY-\alpha$ PHOTONS TRAVEL IS DESCRIBED BY A LARGE NUMBER OF RESONANT SCATTERING THAT CAN HOLD PHOTONS INSIDE A GAS BLOB MEANWHILE THE IONIZING RADIATION CHANGES THE NEUTRAL HYDROGEN DISTRIBUTION. ANOTHER SIGNIFICANT PROBLEM IS THAT FOLLOWING EVERY $LY-\alpha$ PHOTON MAKES THE CODE VERY SLOW. OUR SOLUTION TO BOTH PROBLEMS IS A STATISTICAL APPROACH BASED ON PRE-COMPILED TABLES, WHICH ALLOW US TO BE VERY RAPID AND TO TREAT BOTH RADIATIONS AT THE SAME MOMENT.

CRASH

CODE FOR CONTINUUM RADIATIVE TRANSFER BASED ON MC SAMPLING.

THE RADIATION IS DISCRETIZED IN POLYCHROMATIC PHOTON PACKETS.

THE TIME IS DRIVEN BY THE EMISSION OF PACKETS AND DISCRETIZED IN TIME UNIT.

CIARDI ET AL. (2001), MASELLI, FERRARA & CIARDI (2003), MASELLI, CIARDI & KANEKAR (2008)

McLy α

CODE FOR $LY-\alpha$ RADIATIVE TRANSFER BASED ON MC SAMPLING AND DESIGNED WITH THE SAME STRUCTURE OF CRASH.

THE RADIATION IS DISCRETIZED IN PHOTONS.

THERE IS NO TIME EVOLUTION.

VERHAMME, SCHAEERER & MASELLI (2006)

CRASH α

THE CODE KEEPS THE PACKETS FORMALISM FOR THE CONTINUUM RADIATION.

THE PHYSICAL TIME IS STILL DRIVEN BY IONIZING PACKETS.

STATISTICAL TREATMENT FOR $LY-\alpha$ SCATTERING.

IT IS NOT POSSIBLE TO FOLLOW EVERY SINGLE PHOTON SCATTERING BECAUSE OF THE HUGE COMPUTATIONAL TIME.

THE CODE USES PRE-BUILT TABLES, COMPILED WITH $McLY\alpha$, FOR THE TREATMENT OF THE SCATTERING INSIDE EVERY CELL.

$LY\alpha$ PHOTONS EVOLVE ALONG THE TIMELINE DICTATED BY THE IONIZING RADIATION.

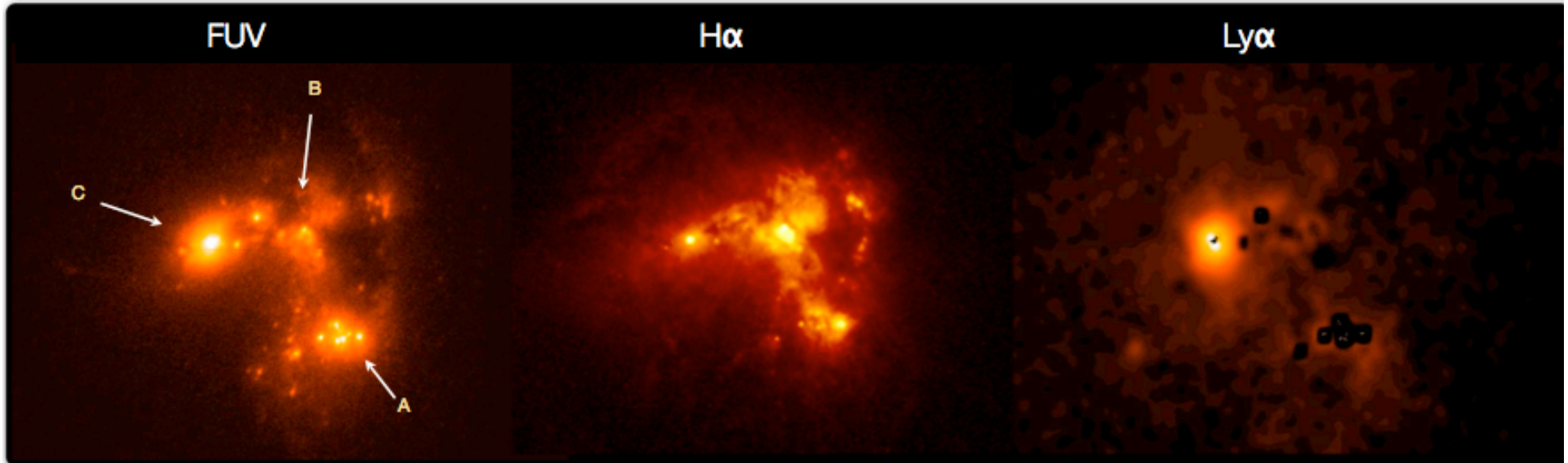
On the Reliability of Lyman-alpha Emission Line as a Cosmological Tool

Hakim Atek (1), Daniel Kunth (1), Matthew Hayes (2), Goeran Ostlin (3), J. Miguel Mas-Hesse (4)

(1) Institut d'Astrophysique de Paris, France
(2) Observatoire de Geneve, Switzerland



(3) Stockholm observatory, Sweden
(4) Instituto d'astrobiologia CSIC-INTA, Madrid, Spain



Dust extinction corrections for Lyman-alpha are tricky

P15

P26: Deep VLT spectroscopy of Ly α envelopes around z=4.5 RQQs

P. North, F. Courbin, A. Eigenbrod (EPFL) & D. Chelouche (IAS) **P26**

Purpose:

answer such questions as:

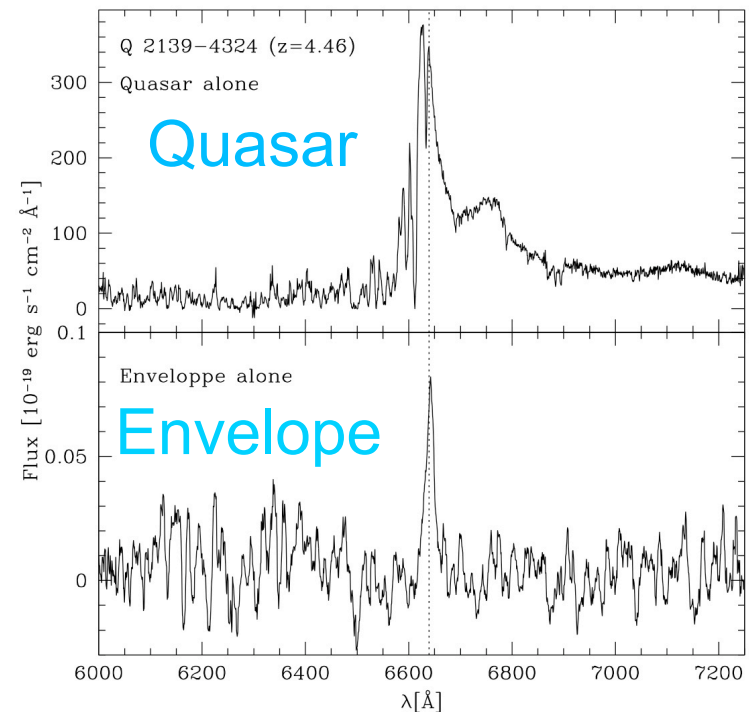
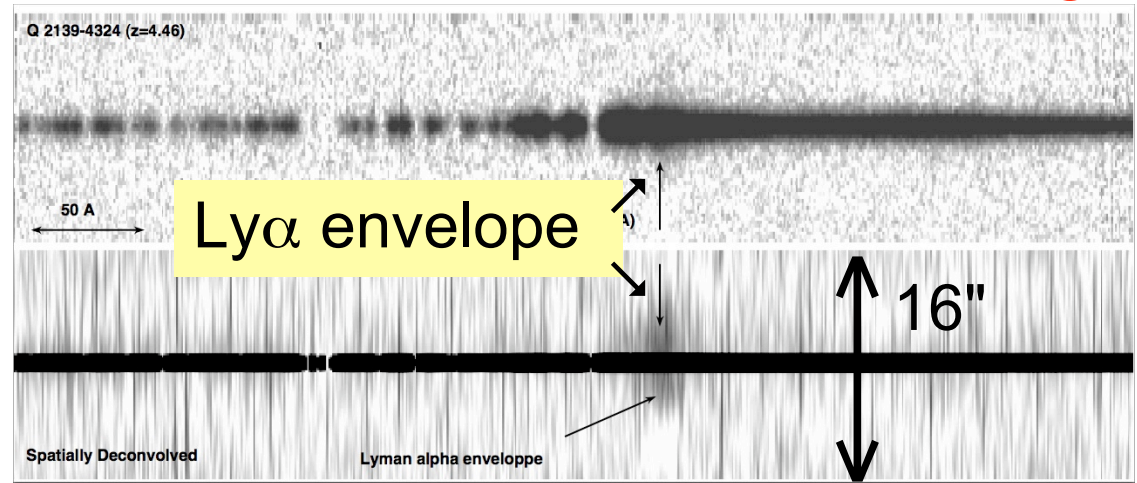
- Frequency of such envelopes?
- Size? Surface brightness?
- Kinematics?
- L(envelope) versus L(QSO)?

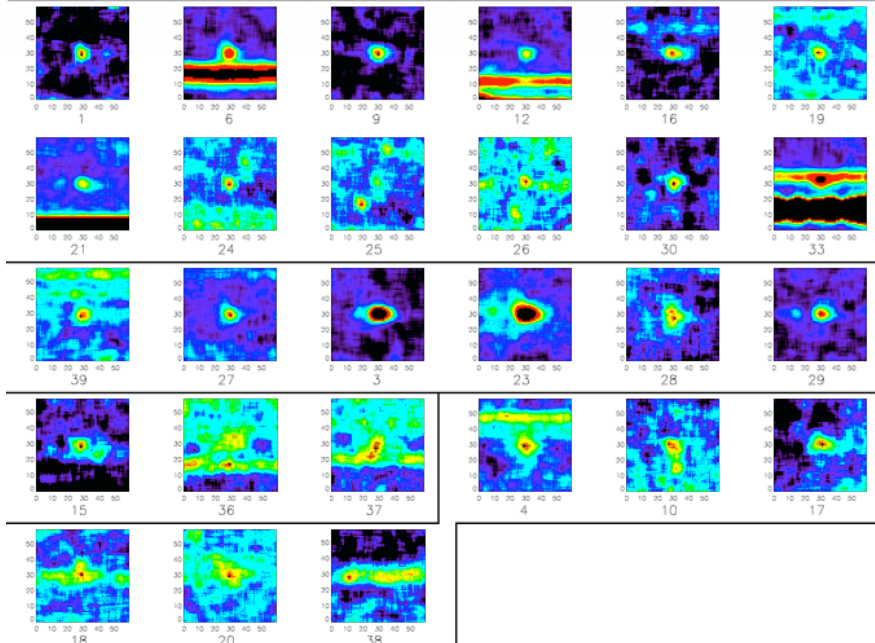
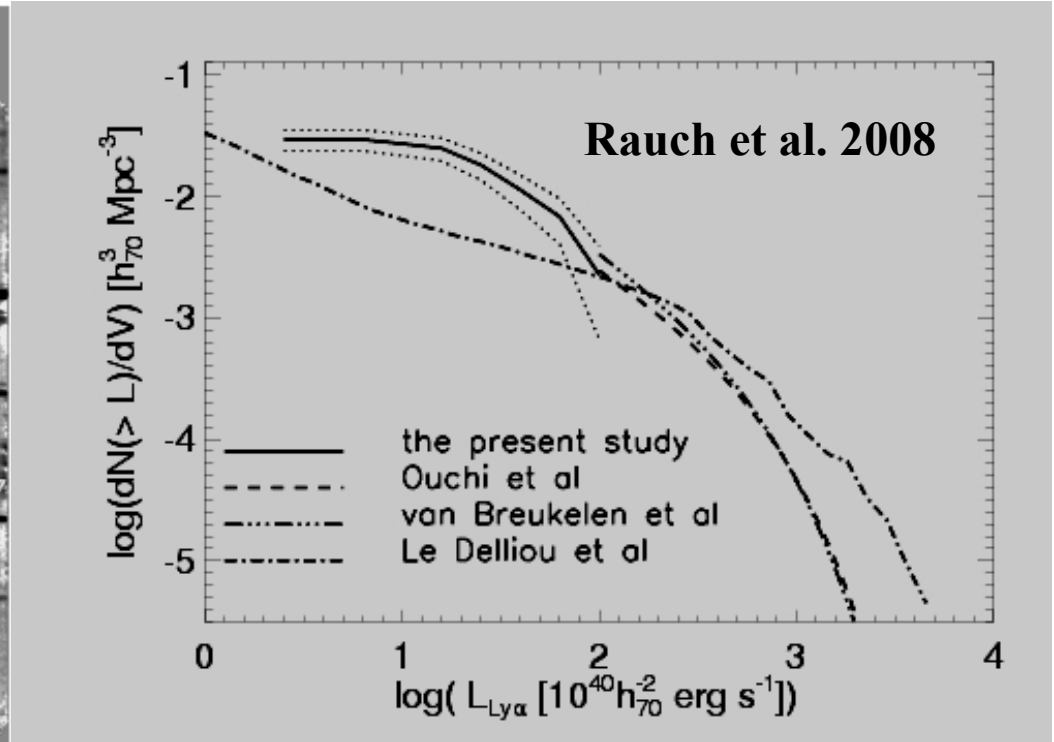
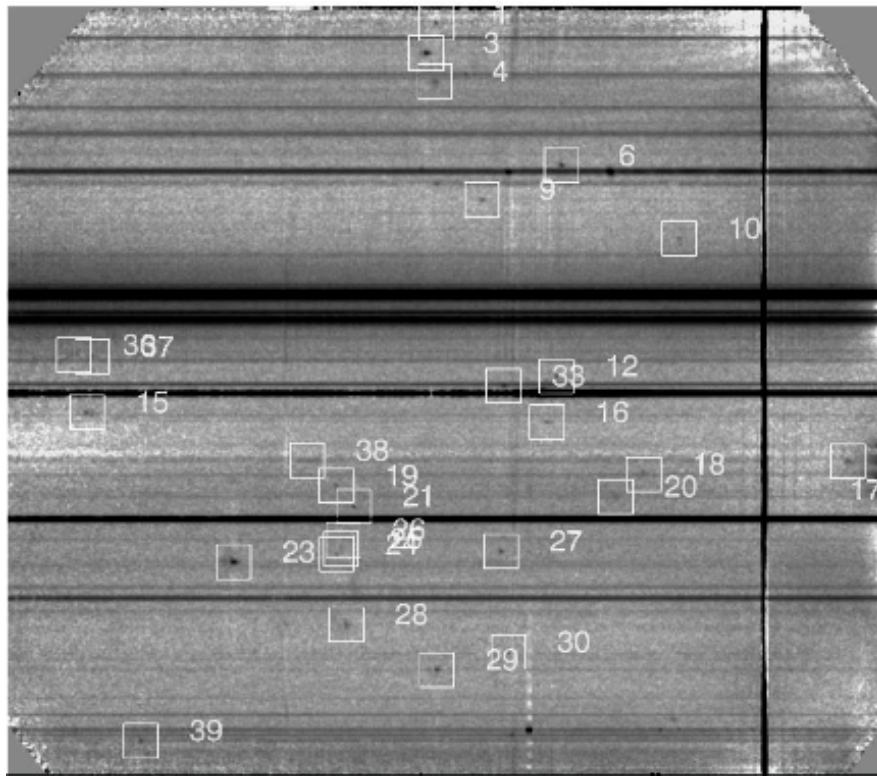
Tools:

- FORS2 in MOS MXU mode:
- $R=1000$, $5200 < t_{\text{exp}} < 10400$ s
- spectral range 600-720 nm
- MCS spatial deconvolution

Results:

- 3 objects observed, 2 envelopes found
- surface brightness LOWER than expected
($\sim 10^{-18}$, $\sim 10^{-20}$ erg s $^{-1}$ cm $^{-2}$ arcsec $^{-2}$)
- Size LARGER than expected!
($\sim 13''$ or 86 kpc ; $\sim 10''$ or 66 kpc)





- 120h with FORS2 sky noise limited
- 27 spatially extended single-line emitters
- The faint end of the luminosity function is very steep!

P00